CLM-P813

Eigenvalues associated with relaxed states of toroidal plasmas

C. G. Gimblett,
J. B. Taylor,
P. J. Hall,
M. F. Turner

UK ATOMIC ENERGY AUTHORITY

Culham Laboratory

CLM-P813

Eigenvalues associated with relaxed states of toroidal plasmas

C. G. Gimblett, P. J. Hall[a)], J. B. Taylor and M. F. Turner

Culham Laboratory, Abingdon, Oxon. OX14 3DB, England
(UKAEA/Euratom Fusion Association)

ABSTRACT

In the theory of relaxed states of toroidal plasmas certain eigenvalues of the equation $\nabla \times \underset{\sim}{B} = \mu \underset{\sim}{B}$ play a crucial role. These eigenvalues are associated with vanishing toroidal flux and determine the onset of current limitation in a toroidal discharge. In axisymmetric systems there are both periodic and axisymmetric eigenfunctions and it is important to know whether the eigenmode associated with the lowest eigenvalue is periodic or axisymmetric. This depends on the shape of the poloidal cross-section and determines the nature of the current limited discharge.

We have computed the eigenvalues of periodic and axisymmetric modes in rectangular and elliptical cross-sections and in re-entrant Multipinch-like cross sections. The re-entrant case required new numerical techniques which are described. We find that in rectangular and elliptic cross-sections the lowest mode is always periodic. However in the Multipinch a transition occurs in which the lowest eigenmode changes from periodic to axisymmetric as the "waist" in the cross-section is made narrower. The critical width is determined. These calculations suggest that in the GA Multipinch experiment the current saturated discharge should be axisymmetric - unlike all other existing pinch experiments where it is periodic.

PACS numbers: 52.30.Bt, 52.55.Dy, 52.55.Hc

(Submitted for publication in Physics of Fluids)

Culham Laboratory
United Kingdom Atomic Energy Authority
Abingdon
Oxfordshire OX14 3DB

March 1987

I. INTRODUCTION

According to the theory of relaxed states[1] a turbulent plasma relaxes to a configuration of minimum energy subject to the constraint of fixed helicity $K = \int \underset{\sim}{A} \cdot \underset{\sim}{B}$. This configuration satisfies

$$\nabla \times \underset{\sim}{B} = \mu \underset{\sim}{B} \quad , \quad \mu = \text{constant} \quad . \tag{1}$$

[For a review of the theory of relaxed states and related experiments see reference 2.]

In a torus the boundary condition $\underset{\sim}{B} \cdot \underset{\sim}{n} = 0$ ensures that the toroidal flux Ψ is also an invariant and the relaxed state is fully determined by the two invariants K and Ψ . However, in order to select the correct, minimum energy, solution of Eq. (1) one must consider certain of its eigenvalues. These are values of μ $(= \mu_i)$ at which there are solutions of Eq. (1) for which the toroidal flux vanishes. We refer to them as "zero-flux" eigenvalues. This zero-flux eigenvalue condition should be distinguished from the better-known condition (in an axisymmetric torus) of vanishing toroidal field at the boundary - required for "field-reversal".

One reason for the importance of the zero-flux eigenmodes is that in a relaxed state μ cannot exeed[2,3] the smallest eigenvalue μ_{min} . This leads to an unexpected and important property of toroidal discharges. It means that, since $\mu = I/\Psi$, there is a maximum toroidal current I (at fixed toroidal flux) in a relaxed state discharge. Below this value the

plasma current increases with Volt-seconds in the discharge, but when the limiting value is reached the current is fixed. Instead of producing higher current any additional Volt-seconds are lost through an increase in plasma inductance. An example of this current limitation is shown in Fig. 1, taken from the Multipinch experiment.[4]

In an axisymmetric torus the zero-flux eigenmodes fall into two distinct classes - those which are themselves axisymmetric and those which are periodic, but not axisymmetric, in the toroidal direction. In the infinite aspect ratio limit which we consider here, the eigenfunctions are $\sim \exp(ikz)$ - with $k = 0$ for the "axisymmetric" class and $k \neq 0$ for the "periodic" class. It is of considerable interest to know whether, for any given cross-section, the lowest eigenfunction is axisymmetric or periodic, for this determines the configuration of the plasma in the current-limited state. It has been observed that current saturation is more clearly evident in experiments where the associated eigenfunction is believed to be axisymmetric (as in Multipinch [4]) than when it is periodic (as in the conventional Reversed Field Pinch[5]). In the latter case there is often no true saturation but only increased resistance and fluctuation levels.[2] This may be because there is much greater plasma-wall interaction in a periodic configuration than in an axisymmetric one.

There is also an interesting theoretical distinction between the two classes of eigenfunction. In a periodic solution the toroidal flux can be written as $\Psi_0 \cdot \exp(ikz)$. However, because of the boundary condition $\underset{\sim}{n} \cdot \underset{\sim}{B} = 0$ the toroidal flux must be independent of z ; consequently Ψ_0 must be zero. Thus, for periodic solutions the boundary condition itself ensures that the toroidal flux vanishes and is sufficient to determine an

eigenvalue. On the other hand, for axisymmetric ($k = 0$) solutions the zero-flux condition must be explicitly imposed in order to determine the eigenvalue*.

A. Some earlier investigations

The first investigation of this problem[1] concerned the simple case of a plasma confined in a circular cylinder of radius a - representing a toroidal discharge of large aspect ratio. For this configuration the lowest zero-flux eigenfunction is a periodic mode

$$B_r = \frac{-1}{(\mu^2 - k^2)^{1/2}} B_0 \left(kJ_1'(y) + \frac{\mu}{y} J_1(y)\right) \sin(\theta + kz) \quad ,$$

$$B_\theta = \frac{-1}{(\mu^2 - k^2)^{1/2}} B_0 \left(\mu J_1'(y) + \frac{k}{y} J_1(y)\right) \cos(\theta + kz) \quad ,$$

$$B_z = B_0 J_1(y) \cos(\theta + kz) \quad , \qquad y = (\mu^2 - k^2)^{1/2} r \quad , \tag{2}$$

with wave number $ka = 1.23$. The corresponding eigenvalue is $\mu a = 3.11$.

---

*The zero-flux eigenvalue problem can be expressed through boundary conditions alone by introducing the vector potential $\underset{\sim}{A}$. Then $\nabla \times \nabla \times \underset{\sim}{A}_i = \mu_i \nabla \times \underset{\sim}{A}_i$ with $\underset{\sim}{A}_i = 0$ on the boundary.

There are an infinite number of other eigenfunctions of the cylindrical system - both axisymmetric ($k = 0$) and periodic ($k \neq 0$) - but all their eigenvalues are greater than 3.11 . The lowest eigenvalue among the $k = 0$ modes is $\mu a = 3.83$. This is actually degenerate and associated with the two distinct eigenfunctions

$$B_r = 0 \ , \quad B_\theta = B_0 J_1(\mu r) \ , \quad B_z = B_0 J_0(\mu r) \ , \tag{3}$$

and

$$B_r = - \frac{B_0}{\mu r} J_1(\mu r)\sin\theta \ , \quad B_\theta = - B_0 J_1'(\mu r)\cos\theta \ , \quad B_z = B_0 J_1(\mu r)\cos\theta \ . \tag{4}$$

Although the lowest eigenmode in a circular cross-section cylinder is periodic, the lowest mode in other cross-sections may be periodic or axisymmetric. This is illustrated by the results obtained for the eigenvalues in Spheromak configurations. [Spheromaks are not true toroidal systems. They are singly-connected and, unlike the toroidal situation, the zero-flux eigenmodes are themselves relaxed states - in fact they are the only relaxed states.[2]] For a Spheromak in the form of a cylinder of height h and radius a the lowest axisymmetric eigenfunction is[6,7]

$$B_r = -B_0(k/\ell)\, J_1(\ell r)\, \cos(kz)$$

$$B_\theta = B_0(\mu/\ell)\, J_1(\ell r)\, \sin(kz)$$

$$B_z = B_0\, J_0(\ell r)\, \sin(kz) \qquad (5)$$

with $kh = \pi$, $\ell a = 3.83$. Its eigenvalue is

$$\mu = \left[\left(\frac{3.83}{a}\right)^2 + \left(\frac{\pi}{h}\right)^2\right]^{1/2} . \qquad (6)$$

The non-axisymmetric, i.e. periodic, modes $\sim \exp(in\phi)$ of this configuration have been obtained numerically.[6,7] The lowest eigenvalue of the $(n = 1)$ mode lies <u>below</u> Eq. (6) when the elongation of the container $h/a > 1.67$. In this Spheromak configuration, therefore, the lowest mode changes from axisymmetric to periodic as the elongation increases. This behaviour illustrates the way in which the relaxed state depends on the shape of the plasma container.

Eigenvalues have also been computed[8] for a "Spheromak with a central conductor". [This is similar to Fig. 2 and is, in fact, a multiply-connected toroidal system!] This computation again implies that the lowest eigenfunction changes from axisymmetric $(n = 0)$ to non-axisymmetric $(n = 1)$ as the height/width of the container is increased. However, it appears that the $n = 0$ mode in this calculation is not associated with the zero-flux eigenvalue condition but with the condition of vanishing toroidal field at the boundary (see Sec. II A).

In the following sections we consider the zero-flux eigenvalues for other forms of flux conserver. In Sec. II we investigate modes in a cylinder with rectangular cross-section (representing the linear analogue of the configuration shown in Fig. 2) using methods similar to those in Refs. 6, 7 and 8. We conclude that the lowest eigenvalue is always associated with a $k \neq 0$ mode whatever the height/width of the cross-section. However, the separation between the lowest $k \neq 0$ mode and the lowest $k = 0$ mode tends to zero as the cross-section becomes more elongated.

In Sec. III we investigate the eigenvalues of configurations with a re-entrant (figure-eight) boundary similar to the Multipinch experiment[4] (Fig. 6). The methods of computation used hitherto are not applicable to such configurations and we have therefore developed two new numerical procedures for computing eigenvalues in cylinders of general cross-section. For the figure-eight cross-section these computations show that the lowest eigenmode changes from periodic to axisymmetric as the "waist" in the cross-section is made narrower and the point at which this transition from periodic mode to axisymmetric mode occurs is computed for the idealised Multipinch configuration.

II. RECTANGULAR CYLINDERS

A. Axisymmetric (k = 0) eigenmodes in a rectangular cross-section cylinder

For axisymmetric modes in a cylinder the magnetic field can be written in the form

$$\underset{\sim}{B} = \underset{\sim}{z} \times \nabla\psi + \underset{\sim}{z}\psi \tag{7}$$

(where $\underset{\sim}{z}$ is along the axis of the cylinder). Then ψ must satisfy

$$\frac{\partial^2\psi}{\partial x^2} + \frac{\partial^2\psi}{\partial y^2} + \mu^2\psi = 0 \tag{8}$$

and must be constant $(= \psi_B)$ on the boundary.

It is convenient to take the rectangular cross-section $0 \leqslant x \leqslant a$, $0 \leqslant y \leqslant b$, then any function $\psi(x,y)$ satisfying the boundary condition can be expressed in the form

$$\psi = \psi_B + \sum a_{mn} \sin\left(\frac{m\pi x}{a}\right) \sin\left(\frac{n\pi y}{b}\right) \tag{9}$$

The a_{mn} must be chosen so that Eq. (8) is satisfied. However, it is necessary to distinguish two classes of potential solutions, according as $\psi_B \neq 0$ or $\psi_B = 0$.

For the first class, with $\psi_B \neq 0$, insertion of (9) into Eq. (8)

leads to a solution

$$\psi = \psi_B \left[1 - \frac{16\mu^2}{\pi^2} \sum_{\substack{\text{odd} \\ m,n}} \frac{\sin\left(\frac{m\pi x}{a}\right) \sin\left(\frac{n\pi y}{b}\right)}{mn(\mu^2 - m^2\pi^2/a^2 - n^2\pi^2/b^2)}\right] . \qquad (10)$$

The toroidal flux associated with this is

$$\Psi = ab\psi_B \left[1 - \frac{64\mu^2}{\pi^4} \sum_{\substack{\text{odd} \\ m,n}} \frac{1}{m^2n^2(\mu^2 - m^2\pi^2/a^2 - n^2\pi^2/b^2)}\right] \qquad (11)$$

and the zero-flux eigenvalues are obtained by setting $\Psi = 0$. A numerical evaluation gives the eigenvalues shown in Fig. 3 (curve a). For a square cross-section $\mu b = 6.79$ and $\mu b \to \pi$ as the elongation $a/b \to \beta$.

When $\psi_B = 0$, each term of the sum in (9) can separately satisfy Eq. (8) and one finds that the second class of solution is

$$\psi = \sin(m\pi x/a) \sin(n\pi y/b) \qquad (12)$$

with

$$\mu^2 = \pi^2\left(\frac{m^2}{a^2} + \frac{n^2}{b^2}\right) . \qquad (13)$$

One might expect from this that the lowest eigenvalue would be

$$\mu^2 = \pi^2\left(\frac{1}{a^2} + \frac{1}{b^2}\right) . \qquad (14)$$

However, this is not a zero flux eigenvalue since the toroidal flux associated with (12) vanishes only if either m or n is even. Consequently the lowest zero-flux eigenvalue among the solutions with $\psi_B = 0$ is not (14) but

$$\mu^2 = \pi^2\left(\frac{4}{a^2} + \frac{1}{b^2}\right) , \qquad (a \geq b) . \tag{15}$$

This result illustrates the importance, referred to in Sec. I, of distinguishing between the zero-flux eigenvalues and those defined by $B_z = 0$ on the boundary. In the present case the latter are given by Eq. (13) for any non-zero m, n, while the former are given by Eq. (13) only when either m or n is even. Thus $m = 1$, $n = 1$ gives the first point at which $B_z = 0$ while $m = 2$, $n = 1$ gives the first zero-flux eigenvalue and the <u>second</u> $B_z = 0$ point. The first $B_z = 0$ point is that associated with spontaneous field reversal.

The eigenvalues obtained from (15) are shown in Fig. 3 (curve b). For a square cross-section $\mu b = 7.02$ which lies just above the value given by (11). However, for cross-sections with an elongation $a/b > 1.12$ the eigenvalue given by (15) is lower than that of (11) but also $\to \pi$ as $a/b \to \infty$.

It will be recalled that in a circular cross-section there are two degenerate eigenmodes with $B_z = B_0 J_0(\mu r)$ and $B_z = B_0 J_1(\mu r) \cos\theta$ respectively. The eigenmodes in the rectangular cross-section which have $\psi_B \neq 0$ are analogous to the $J_0(\mu r)$ mode and those which have $\psi_B = 0$ are analogous to the $J_1(\mu r) \cos\theta$ mode.

B. Periodic ($k \neq 0$) eigenmodes in a rectangular cross-section cylinder

We now consider eigenmodes which are periodic in the z direction, $\sim \exp(ikz)$. In this case it is more convenient to take the rectangular boundary so that $-a/2 \leqslant x \leqslant a/2$, $0 \leqslant y \leqslant b$. The field can no longer be represented in the form (7) but, without loss of generality, it can still be expressed in terms of a single scalar function $\Phi(x,y,z)$ as

$$\underset{\sim}{B} = \underset{\sim}{y} \times \nabla\Phi + \frac{1}{\mu} \nabla \times (\underset{\sim}{y} \times \nabla\Phi) \quad . \tag{16}$$

Then, assuming $\Phi = \mathrm{Re}\left[\phi(x,y)\exp(ikz)\right]$, we have

$$\nabla^2\phi + (\mu^2 - k^2)\phi = 0 \, , \tag{17}$$

and the vanishing of the normal component of $\underset{\sim}{B}$ gives the conditions

$$\frac{\partial^2\phi}{\partial x \partial y} = i\mu k \phi \quad \text{at} \quad x = \pm a/2 \quad \text{for} \quad 0 \leqslant y \leqslant b \tag{18}$$

and

$$\frac{\partial^2\phi}{\partial^2 y} + \mu^2\phi = 0 \quad \text{at} \quad y = 0,b \quad \text{for} \quad -a/2 \leqslant x \leqslant a/2 \quad . \tag{19}$$

By expanding ϕ as a Fourier series, one finds that an expression satisfying the boundary condition (19) must be made up of terms in $\sin\mu y$, $\cos\mu y$ and $\sin(m\pi y/b)$ $(m = 1,2,\ldots)$. We can therefore write a

general expression satisfying Eq. (17) and one pair of boundary conditions in the form

$$\phi = \left(a_0 e^{kx} + b_0 e^{-kx}\right) \cos\mu y + \left(c_0 e^{kx} + d_0 e^{-kx}\right) \sin\mu y +$$

$$+ \sum_{m=1}^{\infty} \left(c_m \cos\lambda_m x + d_m \sin\lambda_m x\right) \sin\left(\frac{m\pi y}{b}\right) , \qquad (20)$$

where

$$b^2\lambda_m^2 = \left((\mu^2 - k^2)b^2 - m^2\pi^2\right) \qquad (21)$$

and a_0 , b_0 , c_m , d_m , are arbitrary coefficients. The problem now consists of satisfying the remaining pair of boundary conditions (18). Re-defining arbitrary coefficients where appropriate, this gives

$$a_0 k e^{kx} e^{-i\mu y} + b_0 k e^{-kx} e^{i\mu y} + \sum_{m=1}^{\infty} ik\left(c_m \cos\lambda_m x + d_m \sin\lambda_m x\right) \sin\left(\frac{m\pi y}{b}\right)$$

$$+ \sum_{m=1}^{\infty} \frac{m\pi\lambda_m}{\mu b} \left(c_m \sin\lambda_m x - d_m \cos\lambda_m x\right) \cos\left(\frac{m\pi y}{b}\right) = 0 \qquad (22)$$

which must be satisfied at $x = \pm a/2$ for $0 \leq y \leq b$.

To make use of (22) we must[6,7,8] express it in a set of functions which are complete over the range $0 \leq y \leq b$. A suitable set is $\left\{\cos\frac{p\pi y}{b} \; ; \; p = 0,1,2\ldots\right\}$. Then we have

$$\sin \frac{m\pi y}{b} = \sum_{p=0}^{\infty} f_{mp} \cos \frac{p\pi y}{b} \qquad (23)$$

where

$$f_{m0} = \frac{1}{m\pi} \left[1 - (-1)^m\right] \; ;$$

$$f_{mp} = \frac{2m}{\pi(m^2 - p^2)} \left[1 - (-1)^{m+p}\right] \quad , \quad p \geq 1 \quad \text{and} \quad m \neq p$$

$$= 0 \qquad , \quad m = p \quad ,$$

and

$$e^{i\mu y} = \sum_{p=0}^{\infty} g_p \cos \frac{p\pi y}{b} \qquad (24)$$

where

$$g_0 = \frac{1}{\mu b} (1 - \cos \mu b)$$

$$g_p = \frac{2i\mu b}{(\mu^2 b^2 - p^2\pi^2)} \left[1 - (-1)^p e^{i\mu b}\right] \quad , \quad p \geq 1 \; .$$

Inserting these expansions into Eq. (22), setting $x = \pm a/2$ and adding and subtracting the results gives (for $p = 1,2,3\ldots$)

$$g_p^* c_0 + g_p d_0 - \frac{p\pi\lambda_p \cot(\lambda_p a/2) d_p}{ik\mu b} + \sum_{m=1}^{\infty} f_{mp} c_m = 0 \qquad (25)$$

$$\tanh\left(\frac{ka}{2}\right)g_p^* c_0 - \tanh\left(\frac{ka}{2}\right)g_p d_0 + \frac{p\pi\lambda_p \tan(\lambda_p a/2)c_p}{ik\mu b} + \sum_{m=1}^{\infty} f_{mp} d_m = 0 \qquad (26)$$

where g_p^* denotes complex conjugate and the coefficients c_m, d_m have again been re-defined. Equations (25) and (26) are an infinite set of linear equations in c_m, d_m and the eigenvalue μ is determined by the requirement that the associated matrix have zero determinant. Taking the complex conjugate of Eqs. (25) and (26) at most only changes the sign of the determinant, which can therefore be taken to be purely real. The eigenvalue is also real.

We have computed approximate eigenvalues by truncating the infinite set of equations (25) and (26) (setting $c_m = d_m = 0$ for $m > M$) and numerically evaluating the resulting determinant. Due to the way the problem is set up (with the boundary condition satisfied algebraically on one pair of walls) the computation of $\mu(a,b,k)$ is quite independent of the computation of $\mu(b,a,k)$. Consequently, a check on the accuracy of the result is provided by the requirement that $\mu(a,b,k) = \mu(b,a,k)$. In most cases this was satisfied to within 10^{-4} with a matrix size of 8×8.

Note that, as discussed earlier, when considering the $k \neq 0$ modes it has not been necessary to introduce the vanishing flux condition explicitly.

The results of the computations of the periodic ($k \neq 0$) modes are summarised in Fig. 3 (curve c) which shows the lowest eigenvalue μ_{min} as

a function of the elongation a/b . The value of the wavenumber k at which this minimum eigenvalue occurs is shown in Fig. 4, and the variation of the eigenvalue with wavenumber is shown in Fig. 5. For a square cross-section the lowest eigenvalue is $\mu b = 5.57$ and occurs at a wavenumber $kb = 2.23$. As the elongation a/b increases the lowest eigenvalue decreases and occurs at a smaller, but always non-zero, wavenumber. In the limit $a/b \to \infty$ (when $\partial\psi/\partial x$ may be neglected) the eigenvalue tends to the limiting value

$$\mu b = (\pi^2 + k^2 b^2)^{\frac{1}{2}} \quad . \tag{27}$$

Figure 3 shows that the lowest eigenvalue among the periodic modes (curve c) always lies below the lowest eigenvalue of both classes of axisymmetric modes (curves a and b) but above the value for field reversal (curve d). However, all four curves approach $\mu b = \pi$ as the elongation $a/b \to \infty$. This means that for rectangular cross-section cylinders the current limited relaxed state would always be periodic (non-axisymmetric) if all values of k are permitted. This might not be so if a "toroidal" periodicity constraint were imposed, and only discrete k are allowed, but, since the permitted values of kb are spaced at intervals of $\sim 2\varepsilon$ (where $\varepsilon = b/2R$ is the toroidal aspect ratio) it can be seen from Figs. 4 and 5 that it is only in systems with large ε and large elongation a/b that the toroidal constraint could be significant.

III. RE-ENTRANT CROSS-SECTIONS

In Sec. II we found that in cylinders with rectangular cross-section the lowest eigenvalue always corresponds to a periodic ($k \neq 0$) eigenmode. As we will show later, the situation is similar for systems with elliptic cross-section.

One might conjecture that for "simple" cross-sections the lowest eigenfunction is always $k \neq 0$. However, the situation may be different for cross-sections which are re-entrant, such as the Multipinch[4] shown in Fig. 6. To understand why, consider the extreme case in which the cross-section is made up of two circles (radius a) connected only by a narrow gap. In this situation an approximate axisymmetric solution of Eq. (1) satisfying the boundary conditions and carrying zero net toroidal flux can be constructed from solutions for the circular cross-section, one in the upper circle carrying positive toroidal flux and one in the lower circle carrying equal, but opposite, flux. Continuity of the field requires that B_z vanishes in the narrow gap and consequently $B_z = 0$ everywhere around the boundary. It is well-known that this occurs when $\mu a = 2.40$, whereas the lowest value of μa at which a periodic eigenmode can be fitted into a circular boundary is $\mu a = 3.11$. This suggests that in a Multipinch-like cross-section the lowest eigenfunction must be axisymmetric ($k = 0$) when the "waist" is very narrow. It also implies that the lowest zero-flux eigenvalue must be close to a value at which $B_z = 0$ on the wall.

The method used to compute eigenvalues for rectangular cylinders in Sec. II cannot be used for other configurations. We have therefore

developed two methods for computing eigenvalues for cylinders of more general cross-section. These are described in the following subsections B 1 and B 2, but we first describe the computation of axisymmetric eigenfunctions in a general cross-section.

A. Axisymmetric Eigenmodes (k = 0)

The computation of $k = 0$ zero-flux eigenfunctions is a straightforward numerical problem, even in highly deformed cross-sections. As in Sec. II A we write

$$\underset{\sim}{B} = \underset{\sim}{z} \times \nabla\psi + \underset{\sim}{z}\phi \quad ; \tag{28}$$

where

$$\frac{\partial^2\psi}{\partial x^2} + \frac{\partial^2\psi}{\partial y^2} + \mu^2\psi = 0 \quad . \tag{29}$$

The boundary condition is ψ = constant ($= \psi_B$) and the zero-flux condition is $\langle\psi\rangle = 0$ (where $\langle\ \rangle$ denotes average over the cross-section). It is convenient to write $\psi = \phi - \langle\phi\rangle$, then one has to solve

$$\nabla^2\phi + \mu^2(\phi - \langle\phi\rangle) = 0 \tag{30}$$

with only the condition ϕ = constant ($= \phi_B$) on the boundary[4]. Since Eq. (30) is unaffected by a change in the origin of ϕ we can set $\phi_B = 0$. The solution of (30) can then be computed by standard methods

such as successive over-relaxation (S.O.R.).

If the boundary is symmetric about the mid-plane, as for Multipinch, the eigenfunctions separate into up-down symmetric (even) modes and up-down antisymmetric (odd) modes. [Note that the terms odd or even refer only to the behaviour in the poloidal plane; all these modes are toroidally axisymmetric.] For any odd mode $\langle\phi\rangle$ vanishes automatically, so ψ is identical to ϕ and $\psi_B = \phi_B = 0$. Hence the odd modes are similar to the second class of $k = 0$ modes found in a rectangular cylinder. Their eigenvalues are also points at which $B_z = 0$ on the boundary. For Multipinch-like cross-sections we find that the lowest axisymmetric zero-flux eigenmode is indeed odd and its eigenvalue coincides with the second value of μ at which $B_z = 0$; the first such value is the conventional "field reversal" point.

B. Periodic Eigenfunctions ($k \neq 0$)

The calculation of $k \neq 0$ eigenmodes in a re-entrant cross-section, proves to be a difficult numerical problem. The origin of this difficulty apparently lies in the need to fit a periodic magnetic field, whose field lines are distorted helices, into a non-periodic but convoluted boundary. The problem can be expressed in the form of a differential equation similar to (17) but the boundary condition is difficult to deal with because it couples the normal and tangential derivatives of ψ. We have developed two successful methods of computation for this problem and these are described in the following subsections.

1. Method 1

Because of the difficulties mentioned above, the method first adopted for finding $k \neq 0$ eigenfunctions in a convoluted cross-section is one which deals directly with the field components B_r, B_θ, B_z. It is restricted to cross-sections in which one can construct a polar co-ordinate system r, θ such that the boundary $r_B(\theta)$ is a single-valued function of θ.

We write the magnetic field in the form

$$B_z(r, \theta, z) = \mathrm{Re}\left[B_z(r, \theta) \exp(ikz)\right] \tag{31}$$

with similar expressions for B_r, B_θ. Then the poloidal dependence of $B_z(r, \theta)$ etc. can be decomposed into terms $\sim \exp(im\theta)$ and the most general magnetic field satisfying Eq. (1) is

$$B_r = \mathrm{Re}\left[\left\{\sum_{m=-\infty}^{\infty} \frac{ir}{y}\left(\frac{\mu m}{y} J_m(y) + kJ_m'(y)\right)a_m e^{im\theta}\right\}e^{ikz}\right]$$

$$B_\theta = \mathrm{Re}\left[\left\{\sum_{m=-\infty}^{\infty} -\frac{r}{y}\left(\frac{mk}{y} J_m(y) + \mu J_m'(y)\right)a_m e^{im\theta}\right\}e^{ikz}\right]$$

$$B_z = \mathrm{Re}\left[\left\{\sum_{m=-\infty}^{\infty} J_m(y) a_m e^{im\theta}\right\}e^{ikz}\right] \tag{32}$$

where $y = (\mu^2 - k^2)^{1/2} r$ and the a_m are arbitrary.

The a_m are to be determined from the condition

$$n_r B_r + n_\theta B_\theta = 0 \tag{33}$$

on the boundary (for all z). This leads to an equation of the form

$$\sum_m a_m f_m(\theta)\, e^{im\theta} = 0 \tag{34}$$

where the functions

$$f_m(\theta) = \frac{r}{2y}\left[(\mu + k)(in_r - n_\theta)J_{m-1}(y) + (\mu - k)(in_r + n_\theta)J_{m+1}(y)\right] \tag{35}$$

must be evaluated at $r = r_B(\theta)$.

We now expand

$$f_m(\theta)e^{im\theta} = \sum_p f_{mp}e^{ip\theta} \tag{36}$$

with

$$f_{mp} = \frac{1}{2\pi}\oint f_m(\theta)e^{i(m-p)\theta}d\theta \ . \tag{37}$$

Then

$$\sum_p \sum_m a_m f_{mp} e^{ip\theta} = 0 \tag{38}$$

so that

$$\sum_m a_m f_{mp} = 0 \quad \text{for} \quad p = 0 , \pm 1 , \pm 2 \ldots \tag{39}$$

This infinite set of equations for a_m is truncated in m and p at $\pm M$ and the determinant of the resulting $(2M + 1) \times (2M + 1)$ matrix is equated to zero in order to determine an approximate eigenvalue $\mu_M(k)$. A value which numerically converges as M is increased is considered to be a satisfactory approximation to $\mu(k)$. A check on the accuracy of this result can be generated by noticing that the condition for vanishing normal field, Eq. (33), can be weighted by an arbitrary function $g(\theta)$. This factor then appears in the integrand of Eq. (37), altering all the matrix elements, but the final $\mu(k)$ should be independent of $g(\theta)$.

If the boundary is symmetrical the computation can be considerably simplified. For the cross-sections considered here,

$$r_B(\theta) = r_B(\pi + \theta) = r_B(\pi - \theta) = r_B(-\theta) \quad . \tag{40}$$

It can be shown that in such cases $\mathrm{Re}(f_{mp}) = 0$ for all m and p, and $f_{mp} \equiv 0$ when $(m - p)$ is odd. Furthermore the symmetry ensures that if $\underset{\sim}{B}(r, \theta)$ is an eigenfunction then $\underset{\sim}{B}(r, \pi + \theta)$ (but <u>not</u> $\underset{\sim}{B}(r, -\theta)$) must also be an eigenfunction. Hence we may again separate the eigenfunctions into even and odd classes, now with $\underset{\sim}{B}(r, \pi + \theta) = +\underset{\sim}{B}(r, \theta)$ and $\underset{\sim}{B}(r, \pi + \theta) = -\underset{\sim}{B}(r, \theta)$ respectively. Clearly even (or odd) eigenfunctions require retention of only even (or odd) values of p. After these reductions the matrix f_{mp} is real and dense. In many cases the

use of a (dense) matrix of order 9×9 gave satisfactory estimates of $\mu(k)$, but it was sometimes necessary to employ a 29×29 matrix. [This requires very accurate evaluation of the Bessel-functions J_m.] In all cases the computation becomes more difficult as the "waist" in the cross-section becomes very narrow.

2. Method 2

In this method we again express the magnetic field in the form

$$\underset{\sim}{B} = \underset{\sim}{z} \times \nabla\psi + \frac{1}{\mu} \nabla \times (\underset{\sim}{z} \times \nabla\psi) \tag{41}$$

with

$$\psi = \psi(x, y) \exp(-ikz) \quad . \tag{42}$$

Then again Eq. (1) is satisfied if

$$\frac{\partial^2\psi}{\partial x^2} + \frac{\partial^2\psi}{\partial y^2} + (\mu^2 - k^2)\psi = 0 \tag{43}$$

and the boundary condition becomes

$$k \frac{\partial\psi}{\partial n} + i\mu \frac{\partial\psi}{\partial s} = 0 \tag{44}$$

where $\partial/\partial n$ and $\partial/\partial s$ are derivatives in the normal and tangential directions respectively.

Writing $\psi = U + iV$ we have

$$\nabla_\perp^2 U + (\mu^2 - k^2)U = 0 \qquad \text{(A)} \qquad (45a)$$

$$\nabla_\perp^2 V + (\mu^2 - k^2)V = 0 \qquad \text{(B)} \qquad (45b)$$

and on the boundary

$$k \left.\frac{\partial U}{\partial n}\right|_B - \mu \left.\frac{\partial V}{\partial s}\right|_B = 0 \qquad (46a)$$

$$k \left.\frac{\partial V}{\partial n}\right|_B + \mu \left.\frac{\partial U}{\partial s}\right|_B = 0 \ . \qquad (46b)$$

Equations (45a) and (45b) can be solved using a standard finite difference scheme on a rectangular (square) mesh in the x-y plane. But for this one needs explicit boundary values for U and V . We therefore first integrate Eqs. (46) around the boundary to give

$$V_B(s) = \frac{k}{\mu} \int_{s_0}^{s} \left.\frac{\partial U}{\partial n}\right|_B ds + V_B(s_0) \qquad \text{(C)} \qquad (47a)$$

and similarly

$$U_B(s) = -\frac{k}{\mu} \int_{s_0}^{s} \left.\frac{\partial V}{\partial n}\right|_B ds + U_B(s_0) \ . \qquad \text{(D)} \qquad (47b)$$

In order for $V_B(s)$ and $U_B(s)$ to be single-valued we must have

$$\oint \frac{\partial U}{\partial n}\Big|_B ds = 0 \quad , \quad \oint \frac{\partial V}{\partial n}\Big|_B ds = 0 \qquad (48)$$

which will be true if

$$\int U \, dxdy = 0 \quad , \quad \int V \, dxdy = 0 \; . \qquad (49)$$

Consequently we must impose these constraints on the solutions of (45a) and (45b).

Once again, symmetry of the cross section simplifies the computation. For the mode with the lowest eigenvalue, U is antisymmetric about $y = 0$ and V is antisymmetric about $x = 0$ so that condition (49) is automatically satisfied. [The remaining description refers specifically to this situation.]

For each k the computation now involves several iteration-loops and also iteration between the four equations A, B, C, and D. An outer iteration involves the functions $U(x, y)$ and $V(x, y)$ and two estimates of the eigenvalue which we designate as μ_u and μ_v. There are also two normalisation constants C_u and C_v. Then the procedure is as follows.

Step 1: Starting from some $V(x, y)$ and μ_v we compute the function U ($= U_B$) on the boundary using Eq. (D). Then by S.O.R. we solve Eq. (A) for $U(x, y)$, iterating on μ to satisfy the normalisation condition (over half the cross-section where $U > 0$)

$$(\mu^2 - k^2) \int U \, dxdy = C_u \, . \qquad (50)$$

[An important point is that each time μ is adjusted in order to satisfy the normalisation, the boundary function U_B is also adjusted according to Eq. (D).] From this iteration emerges $U(x, y)$ and a new value of μ designated μ_u. One then enters Step 2 (which is similar to Step 1 but with U and V interchanged).

Step 2: From $U(x, y)$ and μ_u we compute V $(= V_b)$ on the boundary from Eq. (C) and then solve (B) for $V(x, y)$, iterating to satisfy the normalisation (again over half the cross-section)

$$(\mu^2 - k^2) \int V \, dxdy = C_v \qquad (51)$$

(initially $C_v = C_u$). When this iteration has converged one emerges with $V(x, y)$ and μ_v and returns to Step 1.

After several cycles of iteration between Step 1 and Step 2, it is found that μ_u and μ_v tend to fixed but different values! One then adjusts one of the normalisation constants C_u or C_v to obtain convergence of μ_u and μ_v to a single value μ. Then one has a fully converged solution to the problem and $\mu = \mu(k)$ is the required eigenvalue.

The computations were carried out on a 36×49 square mesh, with some cases being verified on a 72×99 mesh. This required considerably

more computer time than Method 1, but has the advantage of greater flexibility.

C. Application and Results

Before discussing results for the re-entrant cross-sections it is convenient to mention the results obtained for cylinders with elliptic cross-sections. As in the rectangle there are two classes of axisymmetric ($k = 0$) mode, with B_z = zero or non-zero respectively on the wall. The lowest eigenvalue for these two classes (curves a and b), and the lowest eigenvalue for a periodic mode (curve c), are shown in Fig. 7. The value for field reversal is also shown (curve d). The wavenumber k_c corresponding to the lowest periodic eigenmode is shown in Fig. 8. These results confirm that for elliptic cross-sections the lowest eigenmode always occurs at $k \neq 0$ (in agreement with Ref. 9) - as it did for a rectangular cross-section.

For the investigation of Multipinch-like configurations we adopted the idealised form shown in Fig. 9, in which the "waist" is a variable parameter. The configuration is made up of arcs of two unit circles, with centres three radii apart, linked by other circular arcs which intersect tangentially and form the waist. The boundary curve $r_B(\theta)$ and the normals $n_r(\theta)$ and $n_\theta(\theta)$ can be expressed in terms of the half-width Δ of the waist by elementary trigonometry. [Note that $r_B(\theta)$ ceases to be single-valued when $\Delta < 0.43$ and Method 1 cannot then be used.]

The two methods described above were used to compute $\mu(k)$ and the computed values were accepted only when there was satisfactory agreement. Method 1 was also subjected to the internal check referred to in Sec. III B 1 using a weighting function $g(\theta) = 1/r_B^2(\theta)$. Computations for a range of k located the lowest eigenvalue μ_{min} and the corresponding wavenumber $k\ (= k_c)$.

Some typical results are shown in Figs. 10-12. Figure 10 shows the eigenvalue $\mu(k)$ for configurations with three different values of Δ. It can be seen that for the two larger values of Δ the lowest μ occurs at a non-zero wavenumber k. However, for the smallest Δ the minimum μ occurs at $k = 0$. Thus, as anticipated, the Multipinch-like configuration exhibits a transition in which the lowest eigenmode changes from periodic to axisymmetric as the waist is narrowed.

This transition is shown more clearly in Fig. 11 in which the value of the wavenumber $k\ (= k_c)$ corresponding to the minimum μ is shown as a function of Δ. For $\Delta \gtrsim 0.66$ the minimum eigenvalue corresponds to a periodic $(k \neq 0)$ mode whereas for $\Delta \lesssim 0.66$ it corresponds to an axisymmetric $(k = 0)$ mode.

Figure 12 shows the minimum eigenvalue and the field reversal point as a function of Δ. The eigenvalue increases slowly as Δ decreases and the field reversal point lies below the eigenvalue but approaches it as Δ decreases - in agreement with the discussion at the beginning of Sec. III.

IV. SUMMARY AND CONCLUSIONS

We have computed the eigenvalues and eigenfunctions of $\nabla \times \underset{\sim}{B} = \mu \underset{\sim}{B}$, (defined by vanishing toroidal flux) which determine the location and nature of the current-limited relaxed state of axisymmetric toroidal discharges. For the four-fold symmetric cross-sections considered the eigenfunctions fall into three classes: (i) axisymmetric modes in which the toroidal field is non-zero on the boundary; (ii) axisymmetric modes in which the toroidal field vanishes on the boundary; and (iii) even and odd periodic modes. It is important to know whether the lowest eigenfunction is periodic or axisymmetric and to which class it belongs. This depends on the shape of the cross-section.

In a cylinder of rectangular or elliptic cross-section, no matter what its elongation, the lowest eigenvalue always belongs to a periodic mode. The wavenumber of this periodic mode decreases, but remains non-zero, as the elongation increases. Its eigenvalue lies below that of all axisymmetric modes but above the lowest value of μ at which the toroidal field vanishes on the boundary (the field-reversal point). As the elongation of the cross-section tends to infinity, the lowest eigenvalue of all three classes of eigenmode, and the field-reversal point, tend towards a common value of μ.

In a cylinder with re-entrant cross-section such as the Multipinch, the situation is different. If the width Δ at the waist exceeds a critical value then the lowest eigenvalue belongs to a periodic mode, as is does in rectangular and elliptic cross-sections. However, when the

waist is less than this critical value the lowest eigenvalue belongs to an axisymmetric mode with zero toroidal field on the boundary. (This does not represent the usual field-reversal point; it is in fact the second value of μ at which there is zero toroidal field on the boundary.) This transition from a periodic to an axisymmetric lowest eigenmode is illustrated clearly in Fig. 11 which shows the wavenumber of the lowest mode as a function of Δ. For the idealised configuration shown in Fig. 9 the transition from periodic to axisymmetric lowest mode occurs at $\Delta = 0.66$ (i.e. when the waist is 66% of the diameter of the upper and lower chambers).

We estimate that the GA Multipinch experiment, described in Ref. 4, can best be represented in terms of our idealised configuration by a value of $\Delta \sim 0.5$. (Although, of course, the experiment does not conform precisely to the idealised configuration and is of finite toroidal aspect ratio.) This is below the critical value and we therefore expect the lowest eigenmode of the Multipinch to be axisymmetric - unlike orthodox pinch experiments where it is periodic. The location and characteristics of this axisymmetric eigenmode are in good agreement with the properties of the current-limited state observed in the experiment[4] but it has not hitherto been shown that the axisymmetric mode is indeed the lowest eigenfunction.

REFERENCES

a) Department of Mathematics and Statistics, Newcastle-upon-Tyne Polytechnic, Northumberland Road, Newcastle-upon-Tyne

[1] J. B. Taylor. Plasma Phys. and Cont. Fusion Research. Proc. 5th IAEA Conference, Tokyo, Vol. 1, p.161 (1974).

[2] J. B. Taylor. Rev. Mod. Phys. 58, 741 (1986).

[3] T. H. Jensen and M. S. Chu. Phys. Fluids 27, 2881 (1984).

[4] R. J. La Haye, T. H. Jensen, P. S. C. Lee, R. W. Moore, and T. Ohkawa. Nucl. Fusion 26, 255 (1986).

[5] H. A. B. Bodin and A. A. Newton. Nucl. Fusion 20, 1255 (1980).

[6] J. M. Finn and W. M. Manheimer. Phys. Fluids 24. 1336 (1981).

[7] A. Bondeson, G. Marklin, Z. G. An, H. H. Chen, Y. C. Lee and C. S. Liu. Phys. Fluids 24, 1682 (1981).

[8] M. Taguchi, T. Miyazaki and S. Kaneko. Phys. Soc Japan 54, 2163 (1985).

[9] P. B. Parks and C. Chu. Bull. Am. Phys. Soc. 31, 1549 (1986).

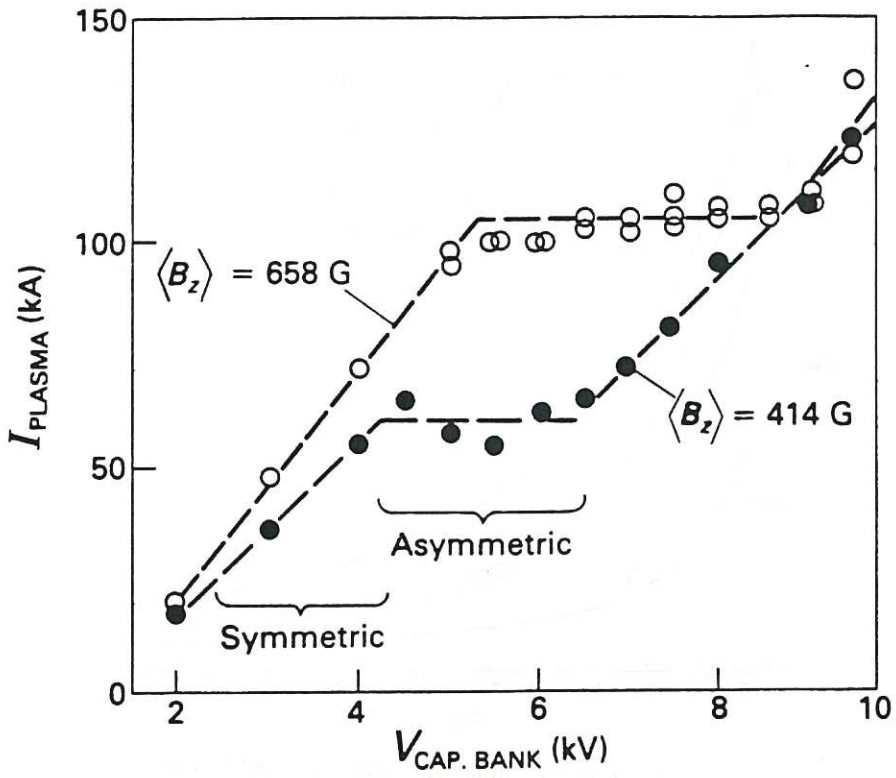

Fig. 1 Current limitation in toroidal discharge (Multipinch, from Ref. 4).

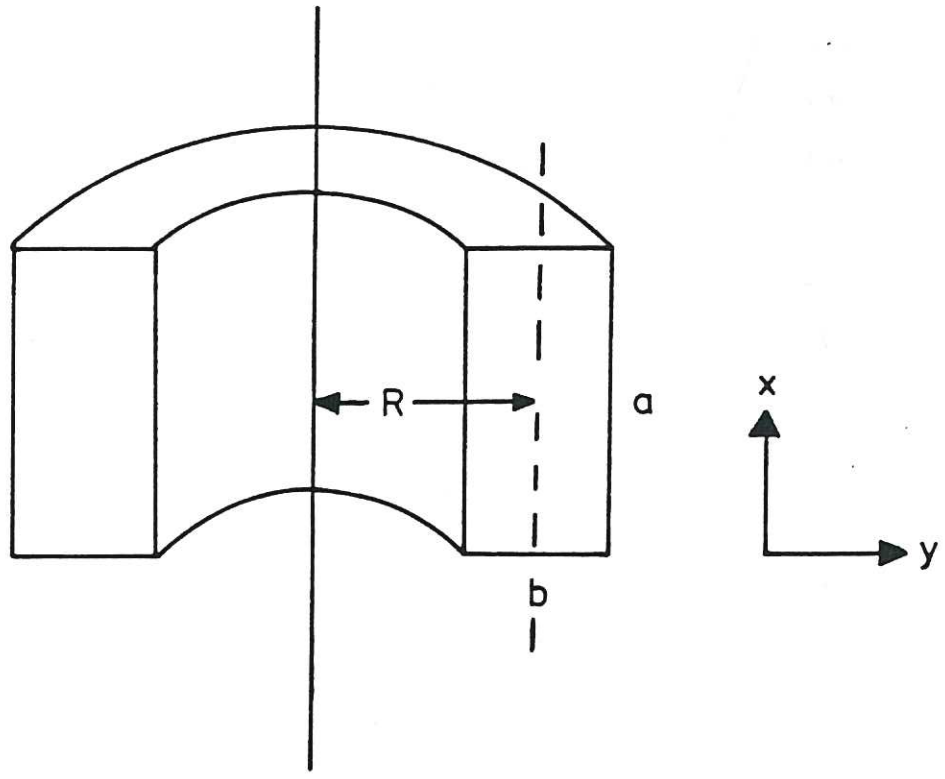

Fig. 2 Rectangular cross-section, toroidal container.

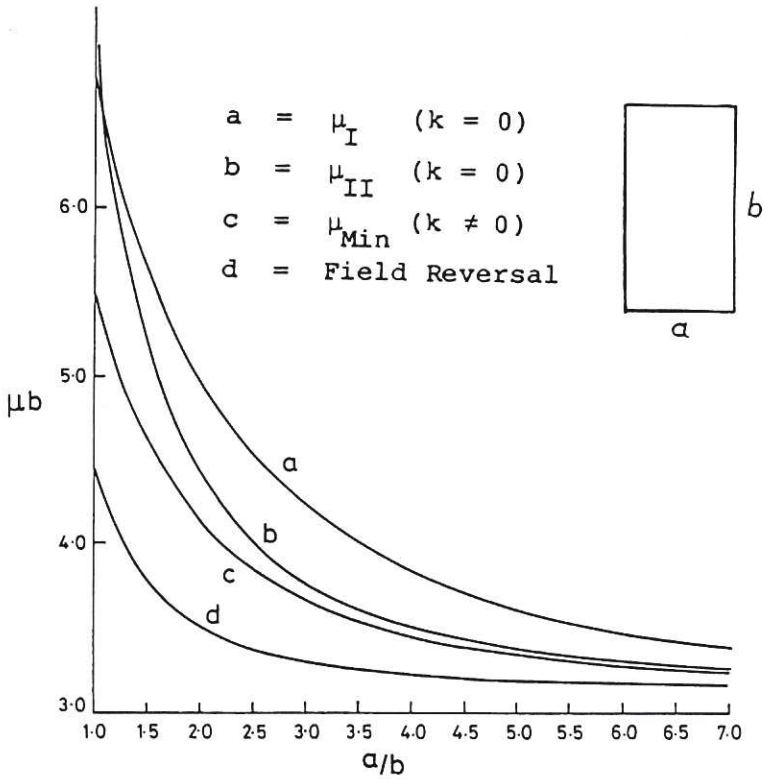

Fig. 3 Eigenvalues for rectangular cross-sections.
(a) Lowest Class I ($\psi_B \neq 0$) symmetric mode.
(b) Lowest Class II ($\psi_B = 0$) symmetric mode.
(c) Minimum eigenvalue, periodic mode.
(d) Field reversal point.

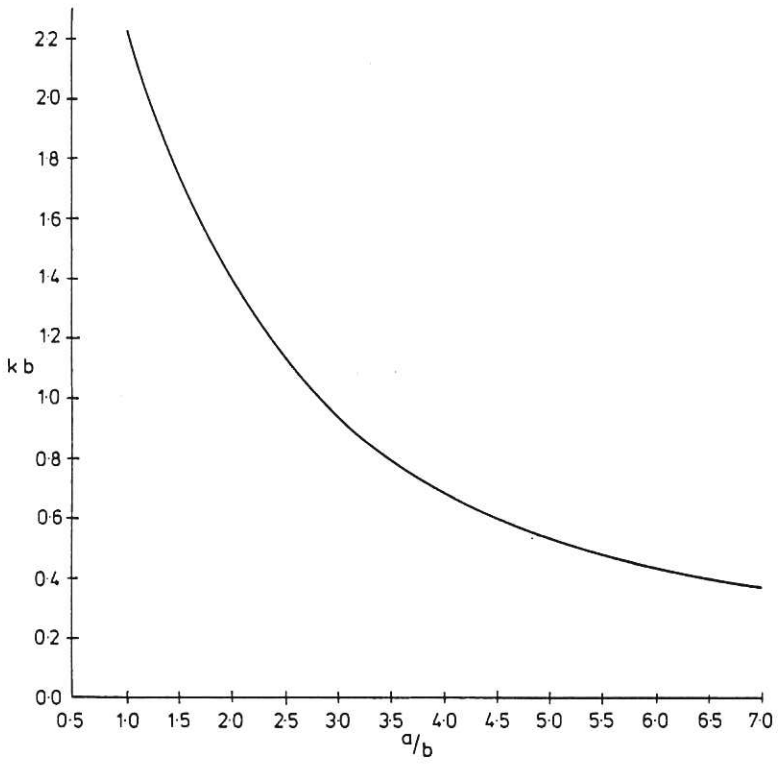

Fig. 4 Wavenumber kb corresponding to minimum eigenvalue in rectangular cross-sections as function of elongation a/b.

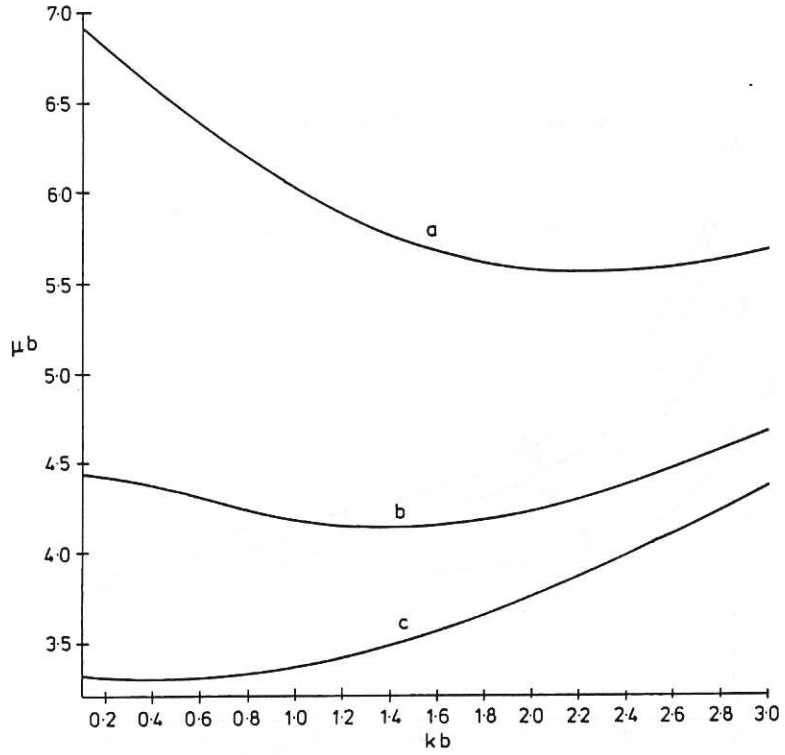

Fig. 5 Variation of eigenvalue with wavenumber kb in rectangular cross-sections.
(a) Elongation a/b = 1.
(b) Elongation a/b = 2.
(c) Elongation a/b = 6.

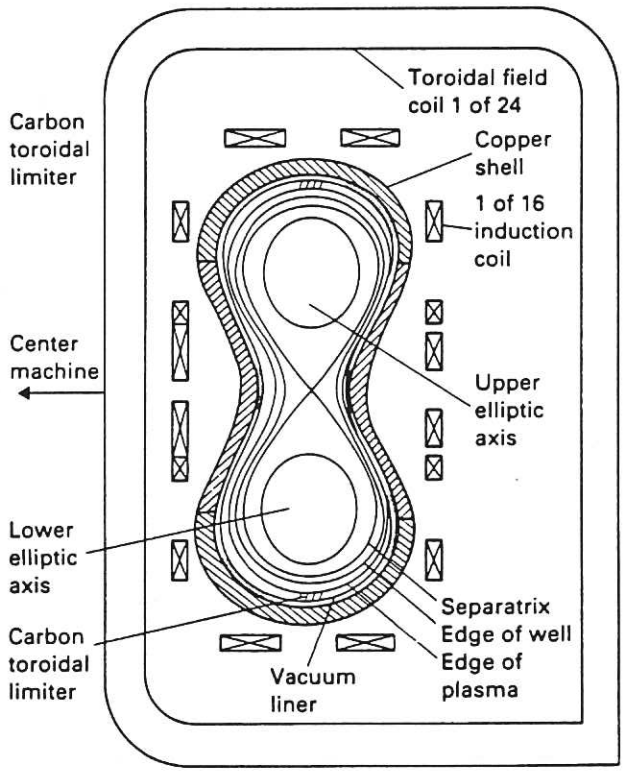

Fig. 6 The Multipinch cross-section (from Ref. 4).

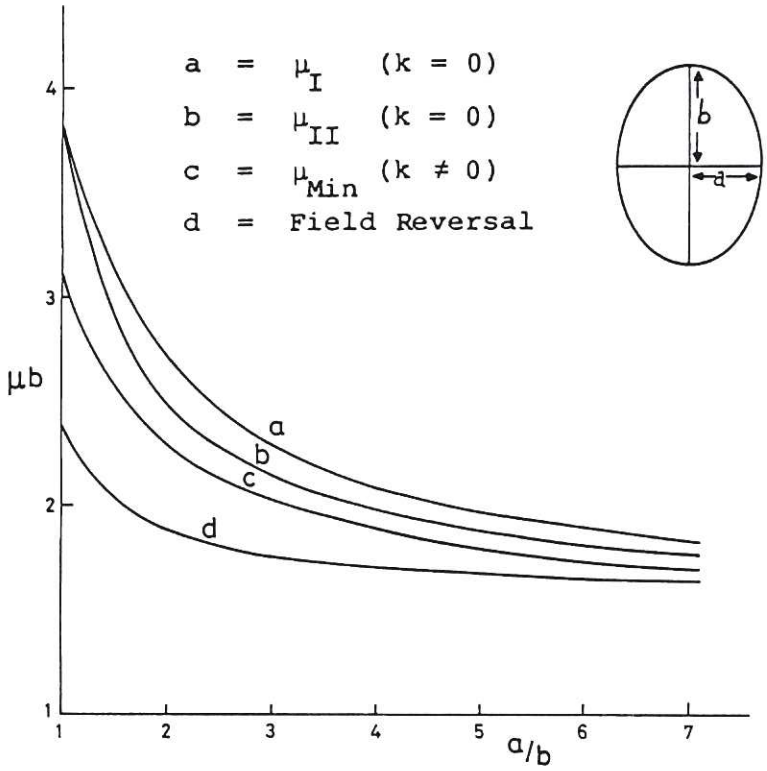

Fig. 7 Eigenvalues for elliptic cross-sections
(a) Lowest Class I ($\psi_B \neq 0$) symmetric mode.
(b) Lowest Class II ($\psi_B = 0$) symmetric mode.
(c) Minimum eigenvalue, periodic mode.
(d) Field reversal point.

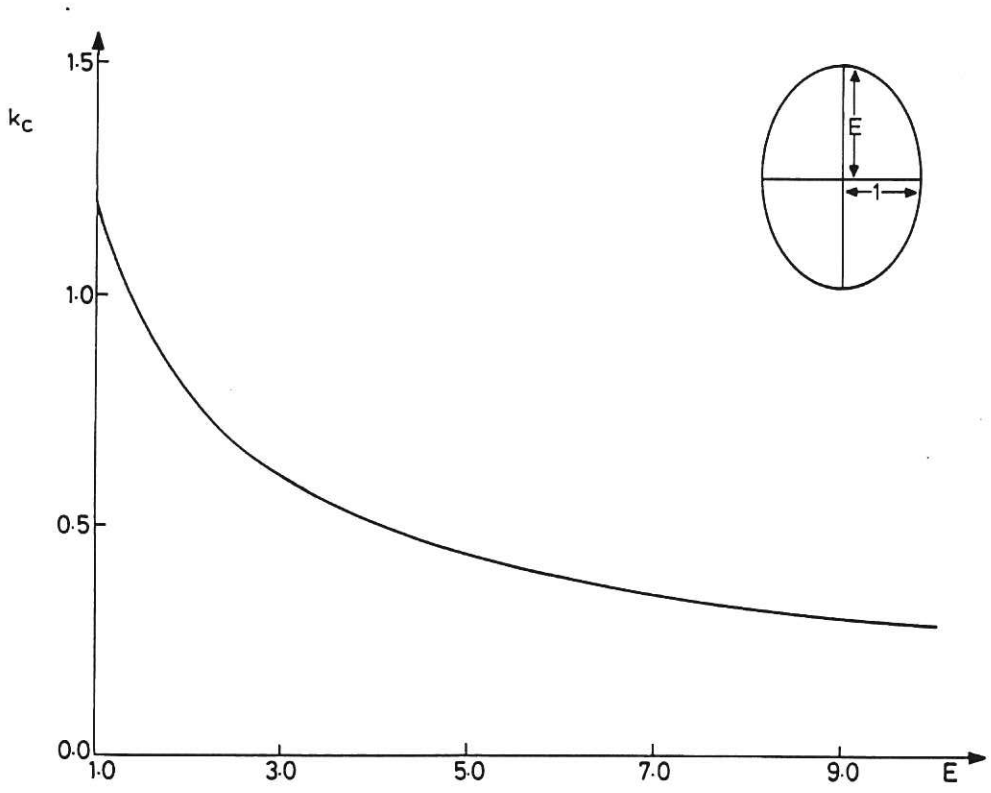

Fig. 8 Wavenumber k_c corresponding to lowest eigenvalue in elliptic cross-section as function of eccentricity.

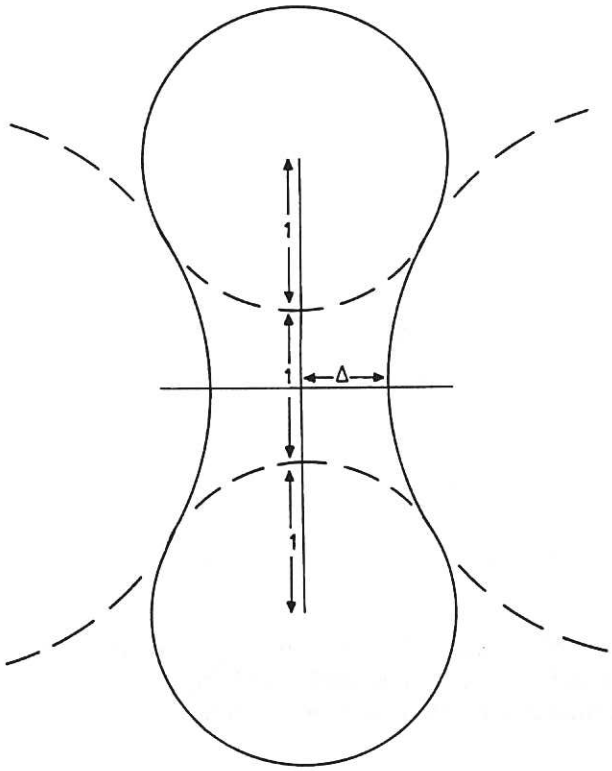

Fig. 9 Idealised Multipinch with variable half-width Δ at waist.

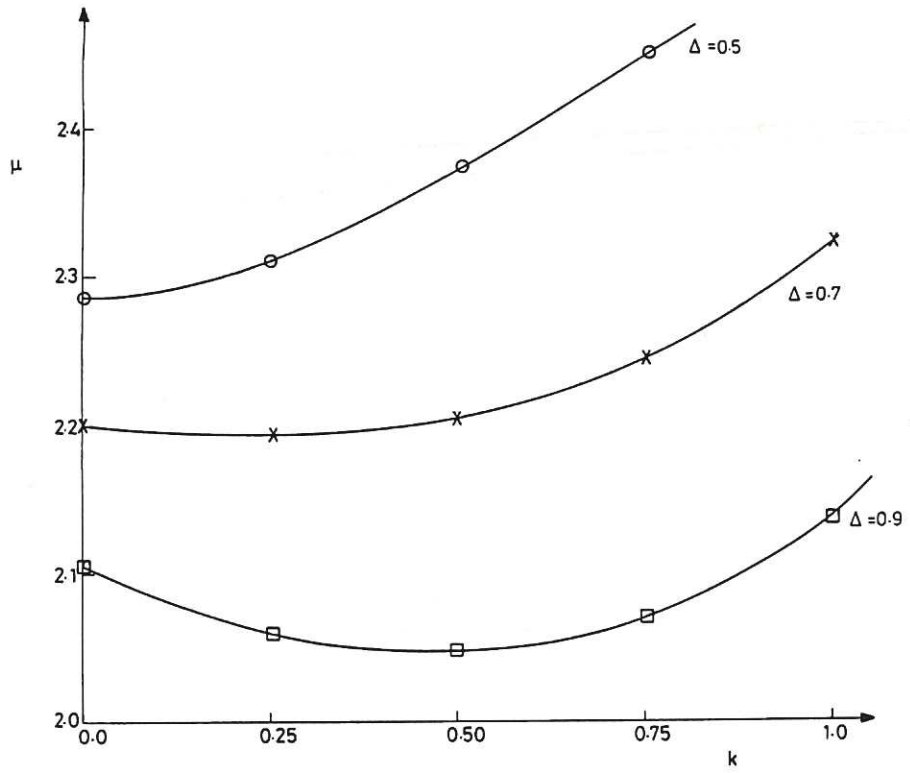

Fig. 10 Eigenvalue μ as function of wavenumber k for idealised Multipinch [for $\Delta = 0.5, 0.7, 0.9$].

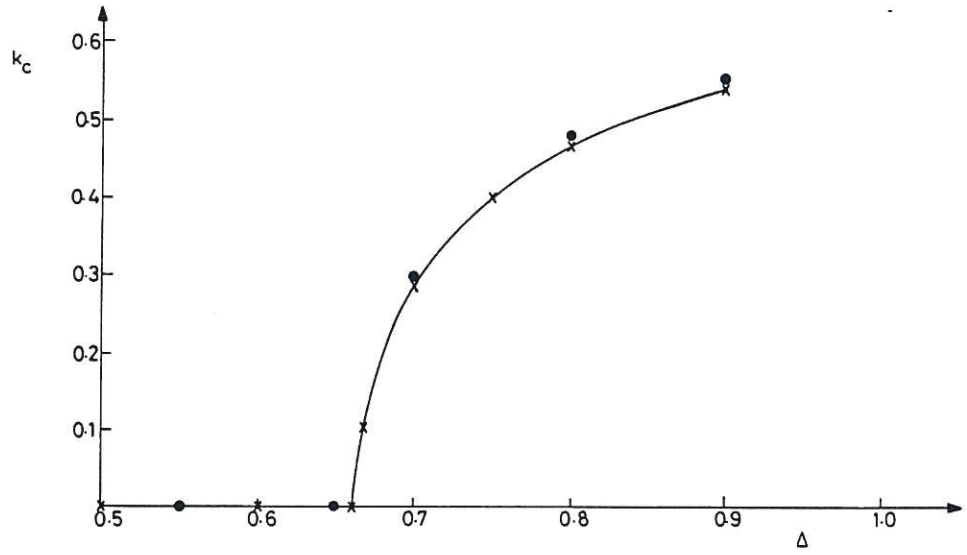

Fig. 11 Wavenumber k_c corresponding to minimum eigenvalue as function of Δ in idealised Multipinch.
x = Computed by Method 1. ● = computed by Method 2.

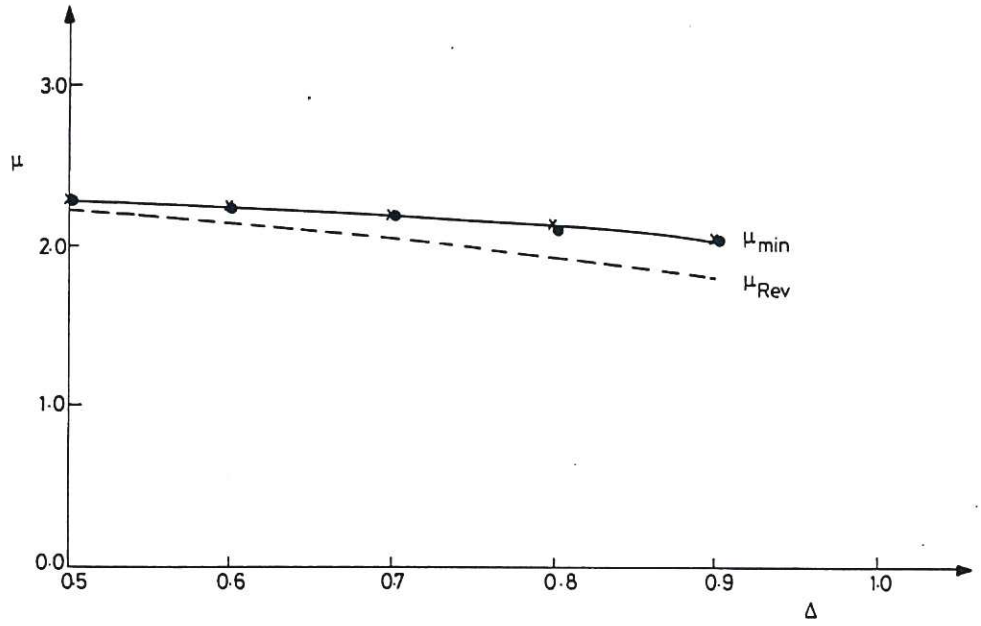

Fig. 12 Lowest eigenvalue μ_{min} and field reversal point μ_{Rev} as function of Δ in idealised Multipinch.
x = Computed by Method 1. ● = computed by Method 2.